

Thermo-Responsive Association of Chitosan-graft-Poly(*N*-isopropylacrylamide) in Aqueous Solutions

Hongqian Bao,[†] Lin Li,^{*,†} Wai Chong Leong,[†] and Leong Huat Gan[‡]

School of Mechanical and Aerospace Engineering, Nanyang Technological University, 50 Nanyang Avenue, Singapore 639798, and Natural Sciences and Science Education, National Institute of Education, Nanyang Technological University, 1 Nanyang Walk, Singapore 637616

Received: June 2, 2010; Revised Manuscript Received: July 15, 2010

A comb-like dual hydrophilic graft chitosan copolymer, chitosan-*graft*-poly(*N*-isopropylacrylamide) (CS-*g*-PNIPAM), was synthesized by means of atom transfer radical polymerization (ATRP) and click chemistry. The thermo-responsive association behavior of the copolymer in dilute aqueous solutions has been investigated by laser light scattering (LLS), zeta potential, and transmission electron microscopy (TEM). The core–shell structured micelles with the hydrophobic PNIPAM as a core and the hydrophilic CS as a shell were formed at low pH (<4) and high temperature (>32 °C), whereas the obtained micelles became large aggregates and precipitated in alkaline solutions (pH > 7). Additionally, the low critical solution temperature (LCST) phase transitions of dense copolymer solutions in the presence of salts (NaCl and NaI) and a cationic surfactant (dodecyltrimethylammonium bromide, DTAB) respectively were studied by micro differential scanning calorimetry (DSC) and UV turbidimetry. It was found that both salts (NaCl and NaI) and DTAB could shift the LCST to lower or higher temperatures from a pure copolymer solution, depending on the beneath mechanisms.

Introduction

Chitosan (CS), as the second most abundant polysaccharide next to cellulose in nature, has attracted much attention in the past decades because of its good biocompatibility, biodegradability, low immunogenicity, and biological activities.^{1–4} With the increasing demand to broaden its application, modification of CS by graft polymerization provides an efficient route to combine the advantages of natural and synthetic polymers. Corresponding to their specific biomedical applications, diverse polymers were grafted to the CS backbone using conventional polymerization techniques and have been well summarized in a few review articles.^{5–8}

Poly(*N*-isopropylacrylamide) (PNIPAM) is one of the most interesting stimuli-responsive polymers, which is water-soluble at room temperature and is able to undergo a coil-to-globule transition above 32 °C (the low critical solution temperature, LCST). PNIPAM-based copolymers have been increasingly employed in various biomedical fields such as drug delivery, tissue engineering, and protein modification, since the LCST of PNIPAM in water is close to body temperature.^{9–11} In recent years, grafting of PNIPAM side chains onto CS constitutes a fast-growing area of research because it makes it possible to achieve both temperature and pH responsive materials which have versatile utilizations. For example, a comb-like CS-*g*-PNIPAM copolymer synthesized by Chen and Cheng was utilized as a cell-carrier for transplantation of chondrocytes and menicus cells for tissue engineering of cartilage.¹² Mao et al. successfully synthesized trimethyl chitosan (TMC)-*g*-PNIPAM which was demonstrated to be a thermo-responsive gene carrier with high transfection efficiency and minimal cytotoxicity.¹³

Using temperature-induced self-assembly and cross-link methods, Chuang et al. fabricated CS-PNIPAM porous nanoparticles and evaluated their special stimuli-sensitive properties and potentials in controlled drug release.¹⁴ Besides their biorelated applications, the rheological properties of CS-*g*-PNIPAM copolymer solutions were investigated by Seetapan and co-workers.¹⁵ In a more detailed manner, Recillas et al. also studied the physicochemical behavior of CS-*g*-PNIPAM solutions by means of micro differential scanning calorimetry (DSC) and dynamic oscillatory high-sensitive rheological measurements.¹⁶ The conventional methods used to synthesize the dual stimuli-responsive graft CS copolymers from the above-mentioned literature can be categorized into the ceric ammonium nitrate (CAN) initiated “grafting from” route and the 1-ethyl-3-(3-dimethylaminopropyl) carbodiimide (EDC) coupled “grafting onto” route. Unfortunately, none of them are applicable to the synthesis of well-defined graft copolymers with side chains that have a narrowly distributed molecular weight.

Atom transfer radical polymerization (ATRP) has been proven to be an attractive means for synthesis of polymers owing to the precise control of molecular weight and polydispersity.^{17,18} In the past few years, the incorporation of the ATRP technique has led to the preparation of many graft CS copolymers with well-defined structures.^{19,20} Considering CS’s poor solubility in most traditional ATRP solvents, the “grafting onto” synthetic route was testified to be superior to the “grafting from” route due to the resultant higher purity and more defined structure.^{21,22} In the meantime, “click” chemistry, as termed by Sharpless et al., gained much attention because of the high specificity, quantitative yield, and near-perfect fidelity in the presence of most functional groups.^{23,24} The beauty and usefulness of click reactions is best demonstrated in the build-up of complex polymeric architectures such as star polymers, multisegmented block copolymers, graft copolymers, dendrimers, and polymer brushes and cross-linked capsules.^{25,26} Click reactions applied

* Corresponding author. E-mail: mlli@ntu.edu.sg. Phone: (+65) 6790 6285. Fax: (+65) 6790 4062.

[†] School of Mechanical and Aerospace Engineering.

[‡] National Institute of Education.

on CS modifications have already been reported in a few publications,^{27,28} but the conception of combining ATRP and click chemistry to prepare well-defined graft CS copolymers via the “grafting onto” technique was first proposed and realized in our recent work.²⁹ Specifically, the “schizophrenic” micelization behavior of the dual hydrophilic graft CS terpolymer, CS(-g-PDMAEMA)-g-PNIPAM in dilute aqueous solutions was systematically investigated.²⁹ The relative infancy of this area means that more research into the synthesis of comb-like copolymers will lead to a greater understanding of structure–property relationships. Driven by this consideration, in this study, we synthesized the well-defined CS-g-PNIPAM brush copolymer by coupling ATRP and click techniques, and characterized it using various techniques. Being different from the pH-responsive stepped association behavior of CS(-g-PDMAEMA)-g-PNIPAM at room temperature,²⁹ the magic thermo-induced association behavior of CS-g-PNIPAM in dilute aqueous solutions is presented in this paper. In addition, the variation of phase transition temperature for the copolymer in dense aqueous solutions in response to some cosolutes (e.g., salts and surfactant) was also studied by micro DSC and UV turbidimetry. We believe that our first obtained information shall serve as a beneficial complement to the existing literature and also help to expand CS’s future applications in the biomedical field.

Experimental Section

Materials. Chitosan ($M_n = 10$ kDa) with an 89% degree of deacetylation (DD, determined by ^1H NMR) was obtained from Haidebei Marline Bioengineering Co., Ltd., China. It was purified according to the method reported in the literature.^{22,30} N-Isopropylacrylamide (NIPAM, 97%, Aldrich) was recrystallized from a mixture of *n*-hexane and benzene (3:1, v/v). Tetrahydrofuran (THF), isopropanol (IPA), and *N,N'*-dimethylformamide (DMF) were dried and distilled prior to use. Ethyl 2-chloropropionate (ECP, 97%), copper(II) chloride (CuCl, 99.995%), sodium azide (Na N_3 , 99%), 2-(*N*-morpholino)ethanesulfonic acid (MES, 99%), sodium L-ascorbate (98%), copper(II) sulfate pentahydrate (CuSO $_4 \cdot 5\text{H}_2\text{O}$, 98%), 4-pentylic acid (95%), *N*-(3-(dimethylamino)propyl)-*N'*-ethylcarbodiimide hydrochloride (EDC·HCl, 99%), *N*-hydroxysuccinimide (NHS, 97%), and other mentioned reagents were purchased from Aldrich and used as received. Tris(2-(dimethylamino)ethyl)amine (Me $_6\text{TREN}$, 98%) was obtained from ATRP Solutions Inc. and directly used.

Synthesis of Azido-Terminated PNIPAM Homopolymer (PNIPAM- N_3). The experiment procedure of the synthesis of PNIPAM- N_3 via ATRP has been described in detail in our recent work,²⁹ and the yield of the synthesis was around 67%. The GPC analysis revealed $M_n = 5600$ g/mol and $M_w/M_n = 1.12$. The actual degree of polymerization (DP) of the PNIPAM block was determined to be 40 by ^1H NMR analysis in D $_2\text{O}$ (comparing the peak area for NIPAM isopropyl at 3.9 ppm with that for the ethoxy at 4.1 ppm). Thus, the homopolymer obtained was denoted as PNIPAM $_{40-N_3}$.

Synthesis of Alkynyl-Pendant CS (alkynyl-CS). The precursor for the click reaction, alkynyl-CS, was prepared by the amidation of CS with 4-pentylic acid in the presence of EDC/NHS. In this case, CS (0.5 g, 2.73 mmol) and 4-pentylic acid (0.054 g, 0.55 mmol) were dissolved in 30 mL of MES buffer (0.1 M, pH adjusted to 5) and degassed. Being protected by argon, EDC (0.32 g, 1.65 mmol) and NHS (0.57 g, 4.95 mmol) were gradually charged into the flask within 20 min. The reaction was conducted at room temperature under stirring for 16 h. To remove impurities, the polymer solution was dialyzed

(MWCO = 3 kDa) against distilled water for 3 days at 4 °C and freeze-dried. The yield was 82% (0.41 g), $M_{n,\text{GPC}} = 10\,800$ g/mol and $M_w/M_n = 1.69$.

Synthesis of CS-g-PNIPAM Copolymer via Click Reaction. To a 50 mL Schlenk flask, alkynyl-CS (0.25 g, 0.1 mmol) and PNIPAM- N_3 (0.9 g, 0.2 mmol) was dissolved in 20 mL of 0.1 M HCl solution and degassed. Under an argon atmosphere, CuSO $_4 \cdot 5\text{H}_2\text{O}$ (0.1 g, 0.4 mmol, in 2 mL of water) and sodium L-ascorbate (0.24 g, 1.2 mmol, in 3 mL of water) were successively added. Then, the pH value of the solution was adjusted to about 6.5 with NaOH solution. The yellow-colored mixture was stirred for 24 h at room temperature. The product was dialyzed (MWCO = 8 kDa) against 0.1% acetic acid for 1 day and against distilled water for 3 days at 4 °C, and then lyophilized into dry powder. The residual PNIPAM homopolymer was removed by extraction with methanol for 24 h in a Soxhlet extractor, and the final product was isolated by filtration and dried under a vacuum (0.53 g, overall yield: 71%).

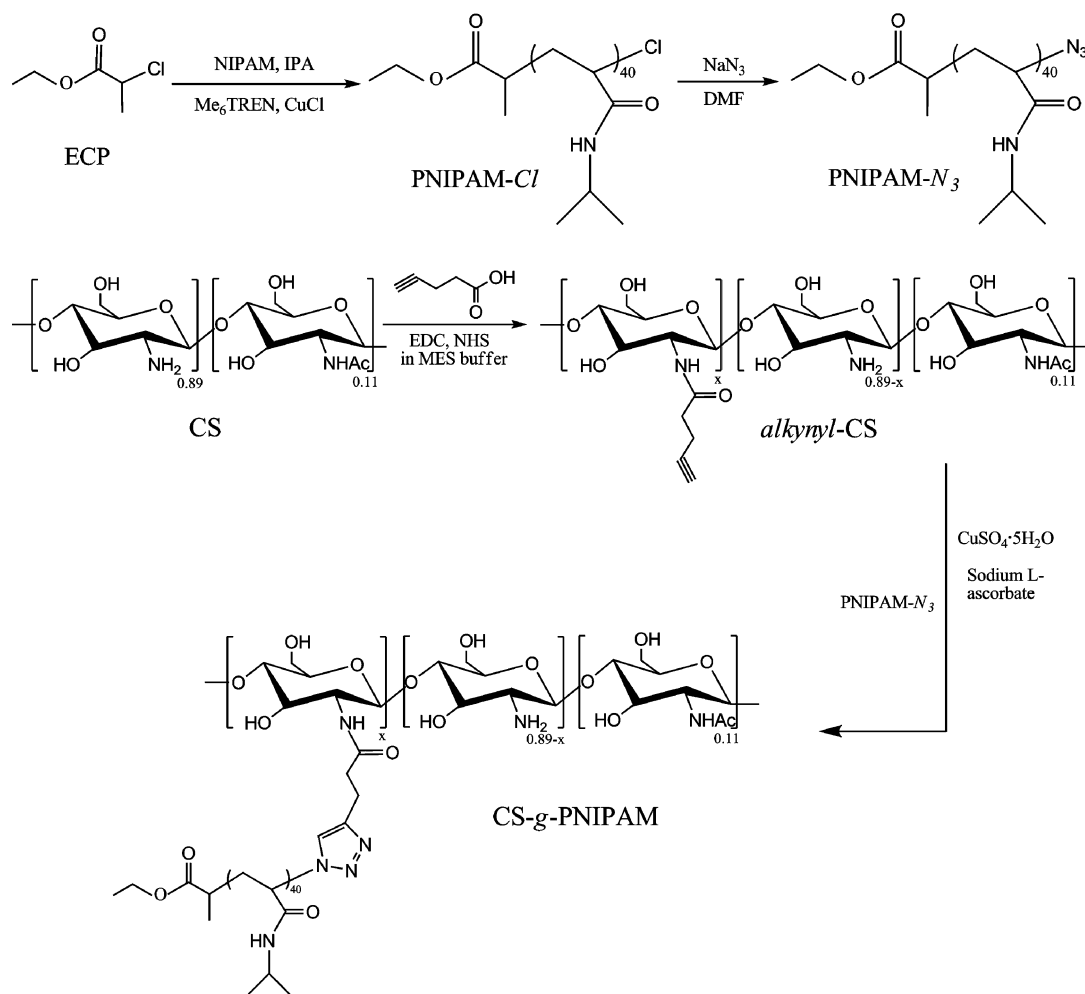
Characterization. The ^1H NMR spectra were recorded using a Bruker DMX-400 spectrometer with CDCl $_3$, D $_2\text{O}$, or D $_2\text{O}/\text{DCl}$ as the solvent. Fourier transformed infrared (FTIR) transmission spectra were obtained on a Perkin-Elmer Spectrum 100 spectrometer by accumulation of 32 scans, with a resolution of 4 cm $^{-1}$. The samples for FTIR were prepared in KBr pellets.

The molecular weight and polydispersity of the polymers were determined using gel permeation chromatography (GPC) at 25 °C. For PNIPAM homopolymers, an Agilent 1100 series GPC system equipped with an LC pump, PL gel columns, and an RI detector were used. The columns were calibrated with polystyrene standards (Agilent EasiCal). The HPLC grade THF containing 0.25% (w/v) tetrabutylammonium bromide (TBABr) was used as a mobile phase for PNIPAM. For CS and its derivatives, the GPC column was replaced by PL aquagel-OH mixed, which was calibrated with pullulan standards. An acetic acid/sodium acetate buffer solution (0.2 M, pH 2.7) was used as the eluent, and the flow rate was fixed at 1.0 mL/min.

The potentiometric and conductometric titrations were carried out on a Metrohm Titrando system equipped with a Conductometer 712. The water jacketed titration vessel was maintained at a constant temperature using a circulating water bath. A 25 mL volume of 0.1 wt % polymer solution was prepared with an excess of 0.05 M HCl and titrated by 0.1 M NaOH under stirring.

Static light scattering (SLS) and dynamic light scattering (DLS) experiments were performed by means of a laser light scattering spectrometer (Brookhaven BI-200SM) equipped with an argon ion laser operating at $\lambda = 488$ nm and a BI9000AT multi- τ digital time-correlator. For SLS, the instrument was calibrated with toluene to ensure that the scattering intensity from toluene had no angular dependence in the testing angular range. For DLS, 90° measurement angle and 3 min correlation measurement time were used as standard parameters. All data were averaged over three measurements. The polymer solutions of 0.02 wt % were prepared and filtered with 0.8 and 0.2 μm filters in tandem prior to the light scattering experiments. The zeta potentials of the colloidal systems with varying pH were characterized by a Brookhaven ZetaPALS analyzer. The measurements were preformed at 40 °C under the Smoluchowski approximation, and three runs of 20 cycles were chosen for a good reproducibility.

The micrograph of the polymer aggregates was taken using a transmission electron microscope (TEM, JEOL JEM-2010) operating at an accelerating voltage of 200 kV. The TEM sample was prepared by dripping a polymer solution onto 400-mesh

SCHEME 1: Synthetic Route of CS-g-PNIPAM via ATRP and Click Chemistry

copper grids precoated with Formvar and stained by 0.2 wt % phosphotungstic acid prior to freeze-drying it.

A UV/vis spectrometer (CARY 50 Bio UV-visible spectrophotometer equipped with a single cell peltier thermo-controller) was used to measure the transmittance (%) of 0.5 wt % copolymer solutions at a wavelength of 500 nm. The temperature range was monitored from 15 to 50 °C, and the LCST was determined from the 50% of the transmittance versus temperature plot.

Calorimetric measurements were carried out on a micro differential scanning calorimeter (VP-DSC, Microcal Inc. MA). A stock solution of 0.5 wt % CS-g-PNIPAM was prepared by dissolving the polymer in 0.1 M acetic acid buffer solution (pH adjusted by adding NaOH), and the weighed cosolutes were then added into aliquot copolymer solutions to give the desired concentration. The thermograms were measured at a heating and cooling rate of 1 °C/min, and the LCST was determined from the peak temperature (T_m) of the endo- or exothermic curve. Standard Hastelloy vessels were used with a calibrated volume of 0.516 mL, and deionized water was used as the reference. Before each test, the sample cell was thoroughly cleaned with a water baseline session to ensure a noncontamination condition.

Results and Discussion

Synthesis of CS-g-PNIPAM Copolymer. As shown in Scheme 1, the major synthesis route was similar to that of our

previously reported synthesis of the graft CS terpolymer.²⁹ The ATRP of NIPAM and subsequent azidation of homopolymer with Na₃N leading to PNIPAM-N₃ were carried out by referring to the literature.³¹ To obtain the alkyne-containing CS derivative, EDC was used to initiate the formation of an amide linkage between 4-pentynoic acid and CS by forming an active intermediate.^{32,33} On the basis of the ¹H NMR spectra of CS and alkynyl-CS (shown in Figure S1 of the Supporting Information), the degree of substitution (DS = 0.074) of alkynyl-CS was determined by the peak integral ratio of resonance signals in the range 2.2–2.5 ppm (methylene protons of the pentynoic group) to that at 2.9 ppm (H₂ of CS). Alternatively, conductometric and potentiometric titration can also help to measure DS by gradually neutralizing protonated amino groups along the alkynyl-CS backbone. The experiment was conducted by titrating 25 mL of 0.1 wt % polymer solution (dissolved in 0.05 M HCl) with 0.1 M NaOH. As shown in Figure S2 of the Supporting Information, the consumed molar amount of titrant NaOH between two inflection points (A and B) for alkynyl-CS is 0.12 mmol. According to the previously reported formula,²⁹ we got $x = 0.066$, which is very close to the DS obtained from ¹H NMR.

In the final step, the synthesis of the CS copolymer was accomplished by the click reaction of alkynyl-CS with PNIPAM-N₃ under mild conditions. In order to guarantee the grafting efficiency, an excess of PNIPAM-N₃ was used to ensure the complete consumption of alkyne moieties, and the removal of

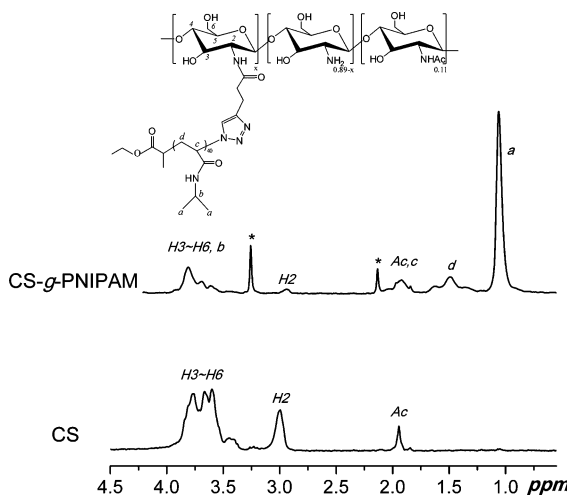


Figure 1. ^1H NMR spectra recorded in D_2O for CS and CS-*g*-PNIPAM.

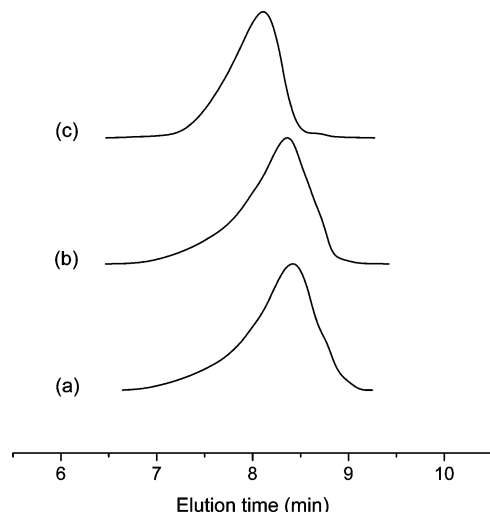


Figure 2. GPC traces for (a) CS, (b) alkynyl-CS, and (c) CS-*g*-PNIPAM in acetic acid buffers.

excess homopolymer was achieved by dialysis and extraction. The FTIR spectrum of the purified product clearly revealed the characteristic absorbance peaks of both components (Figure S3, Supporting Information): 1100 cm^{-1} (C—O stretching) from CS skeletal ether and 2970 cm^{-1} (C—H stretching), 1365 cm^{-1} (C—H bending) from NIPAM methyl groups. From its ^1H NMR spectrum (Figure 1), all characteristic signals of PNIPAM and CS segments can be discerned. The average constitution of the copolymer was determined by calculating the integral ratios between nonoverlapping peaks belonging to each block: H2 at $\delta = 3.1\text{ ppm}$ from CS and methyl protons ($6\text{H}, -\text{CH}-(\text{CH}_3)_2-$) at $\delta = 1.0\text{ ppm}$ from PNIPAM. Assuming that no degradation occurred during the click reaction, the $M_{n,\text{NMR}}$ of the copolymer could reach $30\,000\text{ g/mol}$. The GPC eluograms (Figure 2) indeed show that the graft copolymer has larger $M_n (= 34000\text{ g/mol})$ and smaller $M_w/M_n (= 1.48)$ than those of CS and alkynyl-CS. The low M_w/M_n of the copolymer, indicating a high structural regularity, mainly benefited from the inclusion of narrowly-distributed PNIPAM side chains. The conductometric and potentiometric titration curves of CS-*g*-PNIPAM are shown in Figure 3, and the remarkable reduction in the content of amino groups is not only due to the higher NIPAM monomeric mass in copolymer but also the amidation of amino groups to become alkynyl-CS. On the basis of the above results, we can confirm

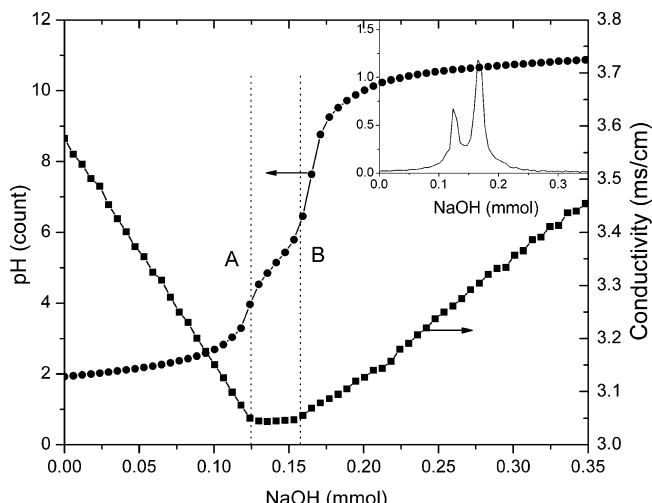


Figure 3. Conductimetric and potentiometric titration curves for 0.1 wt \% CS-*g*-PNIPAM in an excess of 0.05 M HCl solution. The inset represents the difference plot of the pH curve.

the successful synthesis of graft CS copolymer with a well-defined molecular structure. In the subsequent section, the thermo-responsive association behavior of the copolymer in dilute aqueous solutions will be investigated by DLS, SLS, zeta potential, and TEM.

Thermo-Responsive Micellization of CS-*g*-PNIPAM in Dilute Aqueous Solutions. PNIPAM bears both hydrophilic (amide) and hydrophobic (isopropyl and backbone) groups, so water molecules form cage-like structures to surround the hydrophobic moieties of PNIPAM at low temperatures. An increase in temperature will cause the destruction of the “water cages” and the exposure of the hydrophobic groups, leading to the formation of hydrophobic aggregates of PNIPAM. Starting from the unimer state in an aqueous solution at $\text{pH } 4$ and $25\text{ }^\circ\text{C}$, micelles consisting of hydrophobic PNIPAM cores and hydrophilic CS coronas were fabricated upon heating. Figure 4a shows the temperature dependence of intensity-average hydrodynamic radius (R_h) and the dimensionless ratio of gyration radius (R_g) to R_h for the CS-*g*-PNIPAM copolymer at $\text{pH } 4$. It is already known that the theoretical values of R_g/R_h for random coil, core–shell structure, and hard sphere are $1.5, 0.9$, and 0.77 , respectively.^{22,34} Below $30\text{ }^\circ\text{C}$, the graft copolymer molecularly dissolves with D_h remaining invariant around 62 nm . Aggregation starts to form when the temperature exceeds $32\text{ }^\circ\text{C}$, which is accompanied with a sharp increase in R_h and an obviously characteristic bluish tinge of the colloidal dispersion. Above $35\text{ }^\circ\text{C}$, the sizes of the micelles keep almost constant at $\sim 180\text{ nm}$. Synchronously, the value of R_g/R_h decreases from 1.5 to 0.9 while the temperature increases, demonstrating that the copolymer has changed from random coils to core–shell structured micelles. The polydispersities of the aggregates are relatively small ($\mu_2/\Gamma^2 \sim 0.1$), which should be ascribed to the narrow dispersity of the graft chains synthesized via ATRP.²² The actual morphology of the aggregates formed was testified by the TEM micrograph shown in Figure 4b. At $\text{pH } 4$ and $40\text{ }^\circ\text{C}$, spherical micelles with a mean diameter around 150 nm can be identified, which is in good agreement with that determined by DLS considering the hydration effect. At the same time, the uneven darkness distribution in the particles corroborates the formation of core–shell structured micelles.^{14,22}

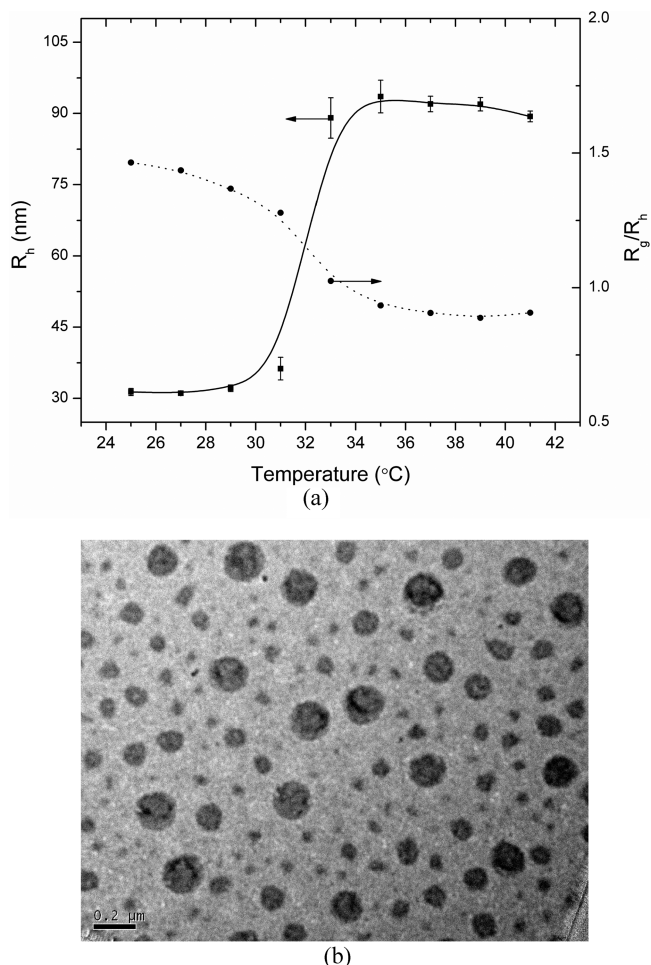


Figure 4. (a) Temperature dependences of R_h and R_g/R_h in aqueous solutions at pH 4 for 0.02 wt % CS-g-PNIPAM micelles. (b) TEM micrograph for self-assembled micelles obtained at pH 4 and 40 °C.

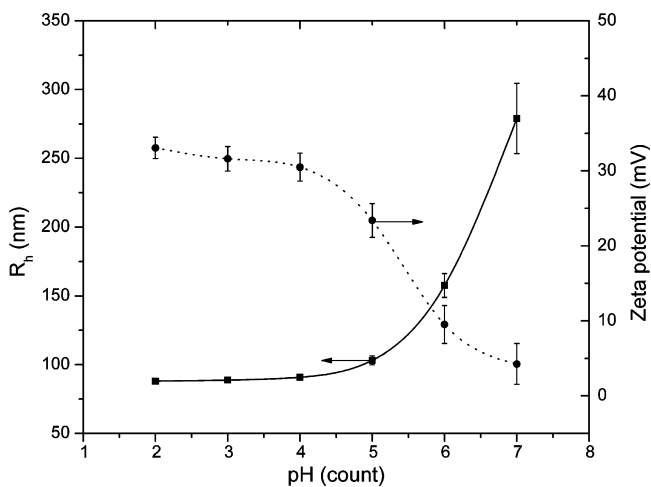


Figure 5. Variations of R_h and zeta potential as a function of pH value at 40 °C for 0.02 wt % CS-g-PNIPAM micelles.

Taking account of the pH sensitivity of CS ($pK_a \sim 5.5$), the particle size and surface charge of CS-g-PNIPAM micelles were also analyzed as a function of pH at 40 °C (Figure 5). Below pH 4, the amino groups on the CS are fully protonated, so the mean particle size keeps stable. Upon addition of NaOH, significant aggregation occurs over pH 5–6, as judged by the dramatic increase in R_h , corresponding to the major deprotonation process of CS. Above pH 7, the white precipitation can

be observed gradually owing to insufficient electrostatic repulsion between micelles' surface to maintain their suspension stability. The change in zeta potential according to pH variation is also displayed in Figure 5: the zeta potential is more than +32 mV at pH < 4, and it decreases continuously to +4.2 mV when the pH is increased to 7.

Cosolute Effects on the LCST of CS-g-PNIPAM in Dense Aqueous Solutions. As described earlier, LSCT is defined as the temperature at which the macromolecules undergo a coil-to-globule transition. The factors that can disrupt the critical balance between the hydrophilic and hydrophobic interactions can affect the LCST. The influence of pH on the thermal transition of CS-g-PNIPAM solutions at 10 wt % acetic acid buffer was recently reported by Recillas et al.,¹⁶ and a similar tendency was confirmed by our work (Table S1, Supporting Information): the LCST decreases while the pH increases from 2.7 to 5.6 despite the COO^- effect. This is because the amino groups in the CS backbone gradually deprotonate when the pH increases. As a result, the balance between electrostatic repulsion and hydrophobic attraction is perturbed, and the increased hydrophobic association leads to phase separation occurring at lower temperature. Since cosolutes such as salts, sugars, and surfactants also affect PNIPAM phase transition, in this work, some representatives were chosen to study their effects on the LCST of CS-g-PNIPAM for the first time.

Effect of Salts on the LCST. According to Hofmeister theory, the effect of salts on the LCST depends on the nature of the salt: salting-in salts accelerate the transition to hydrophobic aggregates and hence lower the LCST, while the salting-out salts enhance the hydrophilicity of the polymer and hence increase the LCST. The Hofmeister series of anions is typically arranged in the following order: $\text{SO}_4^{2-} > \text{H}_2\text{PO}_4^- > \text{F}^- > \text{Cl}^- > \text{Br}^- \sim \text{NO}_3^- > \text{I}^- > \text{SCN}^-$, where the ions on the left are classified as kosmotropes (structure makers) which have strong hydration abilities and exhibit a salting-out effect, while the ions on the right are chaotropes (structure breakers) which have weaker interaction with water molecules and lead to a salting-in effect.^{35,36}

The effect of serial salts on the LCST of PNIPAM has been thoroughly investigated in the past decades,^{37–40} but few articles were found about the combination of PNIPAM with other block polymers. Figure 6a and b illustrates the micro DSC heating curves of the 0.5 wt % CS-g-PNIPAM solutions with different concentrations of NaCl and NaI, and the corresponding LCST values were plotted in Figure 6c. Being consistent with the previous report,¹⁶ a rise in NaCl concentration leads to a continuous decrease in LCST because the introduction of Cl^- ions disrupts the hydrogen bonding effectively between the copolymer and water molecules and results in the dehydration of the copolymer, thus favoring phase separation at lower temperature. On the contrary, the LCST of copolymer solutions with adding I^- ions first reaches a maximum at ~ 0.2 M NaI, and decreases with increasing salt concentration. It is widely accepted that chaotropic anions have two influences on the LCST of PNIPAM: first, the surface tension of the hydrophobically hydrated moieties increases with adding salt (salting-out effect); second, the anions can shed their hydration shells and directly bind to the amide groups (salting-in effect).³⁹ Considering the electrostatic field effect (the largest Debye length at ~ 0.2 M I^-) on the binding, the hydration cages are at the limit of the range of the bound ion influence, which could explain the

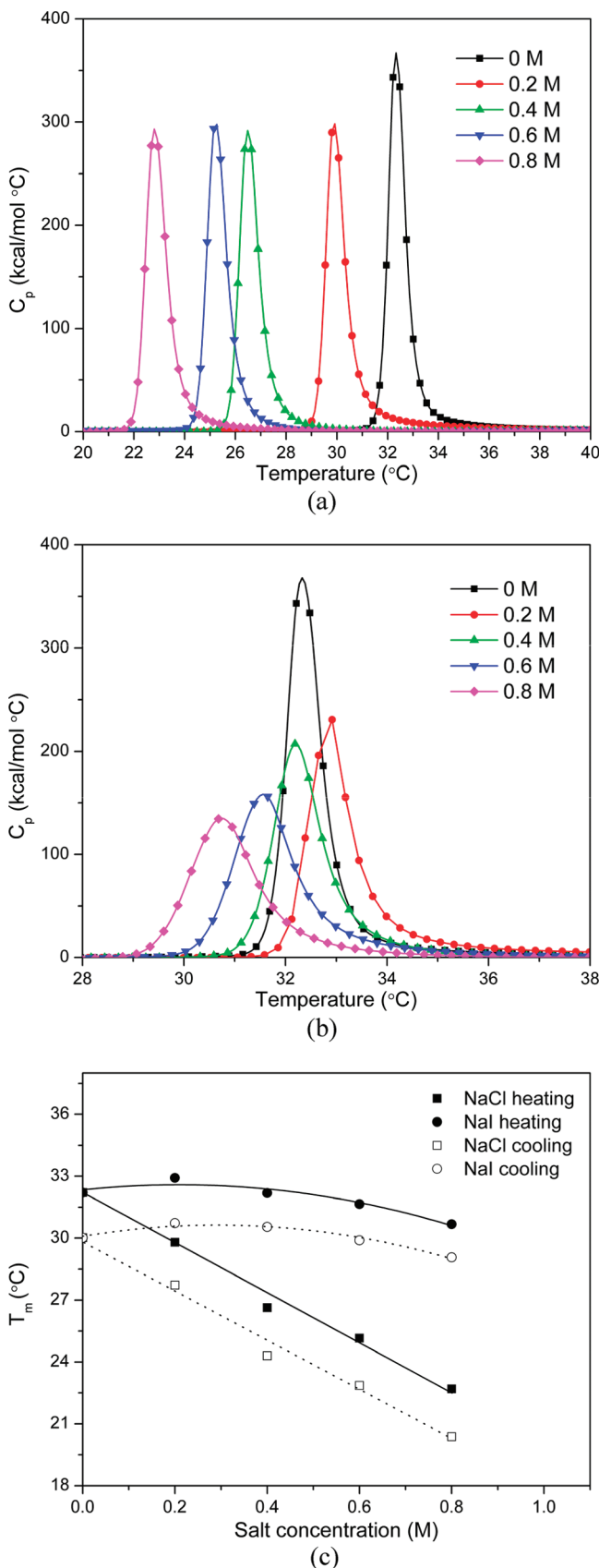


Figure 6. Thermal capacity C_p as a function of temperature during heating process for 0.5 wt % CS-g-PNIPAM solutions containing various concentrations of (a) NaCl and (b) NaI salts. (c) Peak temperatures during phase transition versus salt concentration (M).

diminished binding-induced salting-in effect beyond this concentration.⁴⁰ The lines in Figure 6c represent the theoreti-

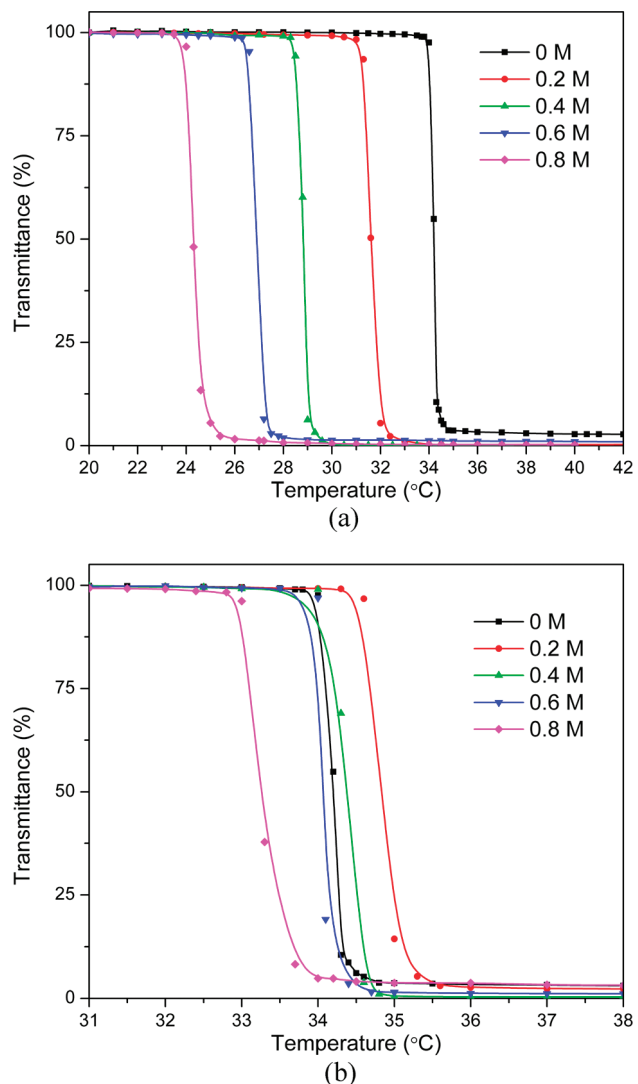


Figure 7. Turbidity behavior of CS-g-PNIPAM solutions during heating process with various concentrations of (a) NaCl and (b) NaI salts at a wavelength of 500 nm.

cal values calculated on the basis of eq 1, which comprises a constant term, a linear term, and a Langmuir isotherm:

$$T = T_0 + c[M] + (B_{\max} K_A [M]) / (1 + K_A [M]) \quad (1)$$

where T_0 is the LCST of PNIPAM in the absence of salt, $[M]$ is the molar concentration of the salt, c (°C/M) is a constant, K_A (M^{-1}) is the apparent equilibrium association constant of the anion with the polymer, and B_{\max} (°C) is the asymptotic increase in LCST due to the anion binding at saturation.^{38–40} The approximate linear curves of LCST versus NaCl concentration reveal the weak binding between Cl^- and the polymer, which is already well corroborated.³⁹ It is also important to note that the endothermic peak (as shown in Figure 6b) becomes lower and broader with rising NaI concentration due to the increased heterogeneous adsorption of the salt on the polymer and decreased cooperativity of the chain collapse. In addition, T_m during the cooling process was about 2 °C lower than that during the heating process, indicating a hysteresis phenomenon which was also previously observed.^{40,41}

The turbidity curves for CS-g-PNIPAM solutions containing NaCl and NaI are presented in Figure 7a and b, respectively.

In all cases, the light transmittance falls sharply in a narrow temperature range until approaching zero, implying that the incident light is mostly scattered by the copolymer's aggregates formed due to the phase separation. The LCST values at various salt conditions determined by DSC and turbidimetry were summarized in Table S2 of the Supporting Information. A similar trend on LCST changes can be identified, and the slight difference in LCST may root in the different determination of LCST using a different method as depicted in our earlier reports.^{41,42} Comparing the concrete LCST data of PNIPAM in the presence of salts, it seems that the incorporation of hydrophilic and positively charged CS segments has a very limited influence on the phase transition of the CS-g-PNIPAM copolymer in aqueous solutions. The main reason should lie on the strong screening effect from the concentrated counterions, and the "neutralized" CS moieties became more hydrophobic and lost electrostatic repulsion even at low pH.

Effect of Surfactant on the LCST. The interaction between polysaccharides (including their hydrophobically modified derivatives) and ionic surfactants in aqueous solutions has been systematically studied in our previous works.^{30,42–44} At the same time, the phase behavior of nonionic PNIPAM in dilute aqueous solutions containing anionic surfactants (e.g., *n*-alkyl sulfates) was also studied by various techniques.^{45,46} In this section, a typical cationic surfactant, dodecyltrimethylammonium bromide (DTAB), was selected to investigate its effects on the LCST of 0.5 wt % CS-g-PNIPAM solutions at pH 4. Since the concentration of Br[−] from the surfactant is lower than 0.07 M in the whole range, the anion effect on the LCST can be ignored according to the former study.³⁹

The micro DSC heating curves of the copolymer solutions as a function of DTAB concentration are shown in Figure 8a, and their peak temperatures are derived in Figure 8b. On the basis of them, three features can be identified: (a) only a single endothermic peak was obtained for each sample; (b) the peak shifts to the left side (lower LCST) of pure CS-g-PNIPAM when the DTAB concentration is ≤ 0.4 wt %, whereas (c) the peak shifts to the right side (higher LCST) when the DTAB concentration is ≥ 0.6 wt %. The cooling curves (not shown) are much more similar to their heating counterparts even though a 2–3 °C hysteresis exists. It is interesting to note that the critical micelle concentration (CMC) of DTAB is 4.8 mg/mL,⁴⁷ which exactly resides in the transition range of 0.4–0.6 wt %. The beneath mechanism is proposed as follows: when the concentration of DTAB is lower than the CMC, the DTAB unimers cooperatively bind to the hydrophobic moieties of PNIPAM and squeeze out their surrounding water molecules, thus facilitating the hydrophobic aggregation. The mixed polymer–surfactant micelles are gradually constructed in the vicinity of the CMC, and the intermolecular polymer–surfactant complexation reinforced with hydrophobic domains of DTAB leads to the minimum LCST; when the DTAB concentration is well above the CMC, the repulsive Coulombic interactions between the ionic heads of DTAB residing in the mixed polymer–surfactant micelles inhibit further collapse of the polymer chains, and those "necklace"-type polymer micelles would become more hydrophilic and render the elevation of the transition temperature.^{30,44,47} Scheme 2 shows a schematic description of the microstructures of CS-g-PNIPAM and DTAB aggregates formed in the different concentration regimes of surfactant.

Coincidentally, Nowakowska and co-workers once reported the analogous phenomenon on the interaction between dodecyltrimethylammonium chloride (DTAC) and copolymers of 2-acryl-

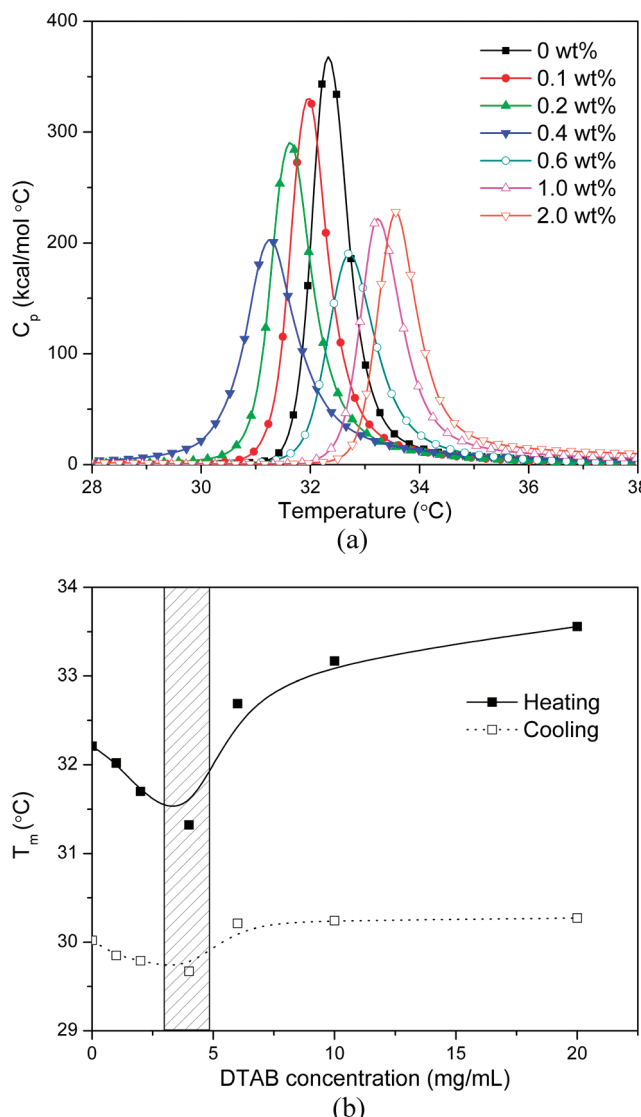
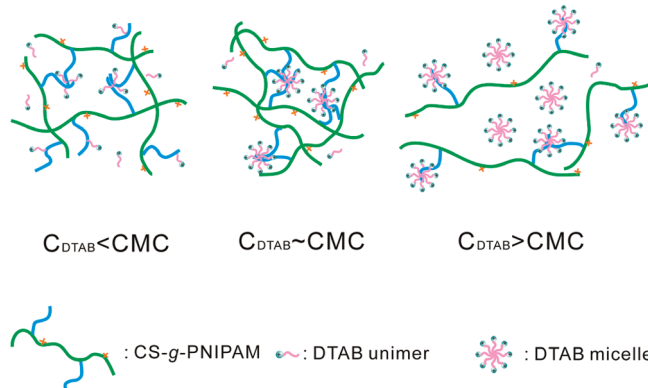


Figure 8. (a) Thermal capacity C_p as a function of temperature during heating process for 0.5 wt % CS-g-PNIPAM solutions containing various concentrations of DTAB. (b) Peak temperatures during phase transition versus surfactant concentration (mg/mL).

SCHEME 2: Schematic Diagram for the Mechanism of DTAB Binding to CS-g-PNIPAM Chains at Different Concentrations of Surfactant



amido-2-methyl-1-propanesulfonate (AMPS) and NIPAM.⁴⁸ They found that the cationic surfactant first bound with the anionic AMPS blocks and decreased the LCST, and for all of the copolymers the minimum LCST was located at a similar

DTAC concentration close to its CMC. Our work enriches the research on the interactions of surfactants with NIPAM-based copolymers by replacing the anionic AMPS with cationic CS segments. Initially, the strong hydrophobic binding of DTAB tails to polymeric chains can reduce the LCST even if electrostatic repulsion exists between DTAB heads and CS protonated amino groups. However, when the mixed micelles and excess free micelles are formed, the repulsive electrostatic forces between them and cationic CS backbones prevail, leading to higher LCST values than these of a copolymer solution free of surfactant (Figure 8b).

Conclusions

In this study, a well-defined and dually stimuli-responsive graft copolymer, CS-g-PNIPAM, has been successfully synthesized via the combination of ATRP and click reaction techniques, as characterized by the ¹H NMR, FTIR, and GPC analyses. The thermo-induced self-assembly behavior of the copolymer in dilute solutions was subsequently investigated by LLS, zeta potential, and TEM. At elevated temperatures (>32 °C), the core–shell structured micelles with PNIPAM as a core and ionized CS as a shell were formed in an acidic environment (pH ~4). With increasing pH at 40 °C, the uniform micelles turned into larger aggregates gradually and precipitated at pH 7. Furthermore, the cosolute effects on the LCST phase transition of the concentrated CS-g-PNIPAM solutions were also studied by micro DSC and UV turbidimetry apparently for the first time. With the addition of a chaotropic salt NaI, the LCST first shifted to higher temperature (salting-in) and then to lower temperature (salting-out). A reverse phenomenon took place when mixing a cationic surfactant DTAB into copolymer solutions. On the basis of different binding mechanisms, their influences on the phase transition of CS-g-PNIPAM in aqueous solutions were comparatively presented and discussed.

Supporting Information Available: Figures showing additional FTIR, conductometric and potentiometric titration, and ¹H NMR results of CS derivatives and tables including the LCSTs of CS-g-PNIPAM under different aqueous conditions. This material is available free of charge via the Internet at <http://pubs.acs.org>.

References and Notes

- (1) Illum, L. *Pharm. Res.* **1998**, *15*, 1326–1331.
- (2) Mao, H.-Q.; Roy, K.; Troung-Le, V. L.; Janes, K. A.; Lin, K. Y.; Wang, Y.; August, J. T.; Leong, K. W. *J. Controlled Release* **2001**, *70*, 399–421.
- (3) Paul, W.; Sharma, C. P. *STP Pharma Sci.* **2000**, *10*, 5–22.
- (4) Kim, I.-Y.; Seo, S.-J.; Moon, H.-S.; Yoo, M.-K.; Park, I.-Y.; Kim, B.-C.; Cho, C.-S. *Biotechnol. Adv.* **2008**, *26*, 1–21.
- (5) Jenkins, D. W.; Hudson, S. M. *Chem. Rev.* **2001**, *101*, 3245–3274.
- (6) Jayakumar, R.; Prabaharan, M.; Reis, R. L.; Mano, J. F. *Carbohydr. Polym.* **2005**, *62*, 142–158.
- (7) Kim, T.-H.; Jiang, H.-L.; Jere, D.; Park, I.-K.; Cho, M.-H.; Nah, J.-W.; Choi, Y.-J.; Akaike, T.; Cho, C.-S. *Prog. Polym. Sci.* **2007**, *32*, 726–753.
- (8) Mourya, V. K.; Inamdar, N. N. *React. Funct. Polym.* **2008**, *68*, 1013–1051.
- (9) Yoshida, R.; Uchida, K.; Kaneko, Y.; Sakai, K.; Kikuchi, A.; Sakurai, Y.; Okano, T. *Nature* **1995**, *374*, 240–242.
- (10) Schild, H. G. *Prog. Polym. Sci.* **1992**, *17*, 163–249.
- (11) Meyer, D. E.; Shin, B. C.; Kong, G. A.; Dewhirst, M. W.; Chilkoti, A. *Controlled Release* **2001**, *74*, 213–224.
- (12) Chen, J.-P.; Cheng, T.-H. *Macromol. Biosci.* **2006**, *6*, 1026–1039.
- (13) Mao, Z.; Ma, L.; Yan, J.; Yan, M.; Gao, C.; Shen, J. *Biomaterials* **2007**, *28*, 4488–4500.
- (14) Chuang, C.-Y.; Don, T.-M.; Chiu, W.-Y. *J. Polym. Sci., Part A: Polym. Chem.* **2009**, *47*, 5126–5136.
- (15) Seetapan, N.; Mai-ngam, K.; Plucktaveesak, N.; Sirivat, A. *Rheol. Acta* **2006**, *45*, 1011–1018.
- (16) Recillas, M.; Silva, L. L.; Peniche, C.; Goycoolea, F. M.; Rinaudo, M.; Argüelles-Monal, W. M. *Biomacromolecules* **2009**, *10*, 1633–1641.
- (17) Matyjaszewski, K.; Xia, J. *Chem. Rev.* **2001**, *101*, 2921–2990.
- (18) Kamigaito, M.; Ando, T.; Sawamoto, M. *Chem. Rev.* **2001**, *101*, 3689–3746.
- (19) El Tahlawy, K.; Hudson, S. M. *J. Appl. Polym. Sci.* **2003**, *89*, 901–912.
- (20) Li, N.; Bai, R.; Liu, C. *Langmuir* **2005**, *21*, 11780–11787.
- (21) Munro, N. H.; Hanton, L. R.; Moratti, S. C.; Robinson, B. H. *Carbohydr. Polym.* **2009**, *77*, 496–505.
- (22) Bao, H.; Hu, J.; Gan, L. H.; Li, L. *J. Polym. Sci., Part A: Polym. Chem.* **2009**, *47*, 6682–6692.
- (23) Rostovtsev, V. V.; Green, L. G.; Fokin, V. V.; Sharpless, K. B. *Angew. Chem., Int. Ed.* **2002**, *41*, 2596–2599.
- (24) Wang, Q.; Chan, T. R.; Hilgraf, R.; Fokin, V. V.; Sharpless, K. B.; Finn, M. G. *J. Am. Chem. Soc.* **2003**, *125*, 3192–3193.
- (25) Binder, W. H.; Sachsenhofer, R. *Macromol. Rapid Commun.* **2008**, *29*, 952–981.
- (26) Lodge, T. P. *Macromolecules* **2009**, *42*, 3827–3829.
- (27) Kulbokaite, R.; Ciuta, G.; Netopilik, M.; Makuska, R. *React. Funct. Polym.* **2009**, *69*, 771–778.
- (28) Lallana, E.; Fernandez-Megia, E.; Riguera, R. *J. Am. Chem. Soc.* **2009**, *131*, 5748–5750.
- (29) Bao, H.; Li, L.; Gan, L. H.; Ping, Y.; Li, J.; Ravi, P. *Macromolecules* **2010**, *43*, 5679–5687.
- (30) Bao, H.; Li, L.; Zhang, H. *J. Colloid Interface Sci.* **2008**, *328*, 270–277.
- (31) Jiang, X.; Zhang, G.; Narain, R.; Liu, S. *Soft Matter* **2009**, *5*, 1530–1538.
- (32) Sun, S.; Liu, W.; Cheng, N.; Zhang, B.; Cao, Z.; Yao, K.; Liang, D.; Zuo, A.; Guo, G.; Zhang, J. *Bioconjugate Chem.* **2005**, *16*, 972–980.
- (33) Chen, J.-P.; Cheng, T.-H. *Macromol. Biosci.* **2006**, *6*, 1026–1039.
- (34) Rubinstein, M.; Colby, R. H. *Polymer Physics*; Oxford University Press: Oxford, U.K., 2003.
- (35) Xu, Y.; Li, L.; Zheng, P.; Lam, Y. C.; Hu, X. *Langmuir* **2004**, *20*, 6134–6138.
- (36) Xu, Y.; Wang, C.; Tam, K. C.; Li, L. *Langmuir* **2004**, *20*, 646–652.
- (37) Schild, H. G.; Tirrell, D. A. *J. Phys. Chem.* **1990**, *94*, 4352–4356.
- (38) Zhang, Y.; Furyk, S.; Bergbreiter, D. E.; Cremer, P. S. *J. Am. Chem. Soc.* **2005**, *127*, 14505–14510.
- (39) Zhang, Y.; Furyk, S.; Sagle, L. B.; Cho, Y.; Bergbreiter, D. E.; Cremer, P. S. *J. Phys. Chem. C* **2007**, *111*, 8916–8924.
- (40) Shechter, I.; Ramon, O.; Portnaya, I.; Paz, Y.; Livney, Y. D. *Macromolecules* **2010**, *43*, 480–487.
- (41) Xu, Y.; Li, L. *Polymer* **2005**, *46*, 7410–7417.
- (42) Wang, Q.; Li, L.; Liu, E.; Xu, Y.; Liu, J. *Polymer* **2006**, *47*, 1372–1378.
- (43) Bao, H.; Li, L.; Gan, L. H.; Zhang, H. *Macromolecules* **2008**, *41*, 9406–9412.
- (44) Li, L.; Liu, E.; Lim, C. H. *J. Phys. Chem. B* **2007**, *111*, 6410–6416.
- (45) Meewes, M.; Ricka, J.; De Silva, M.; Nyffenegger, R.; Binkert, T. *Macromolecules* **1991**, *24*, 5811–5816.
- (46) Winnik, F. M.; Ringsdorf, H.; Venzmer, J. *Langmuir* **1991**, *7*, 905–911.
- (47) Jönsson, B.; Lindman, B.; Holmberg, K.; Kronberg, B. *Surfactants and Polymers in Aqueous Solution*; John Wiley & Sons: Chichester, U.K., 1998.
- (48) Nowakowska, M.; Szczubialka, K.; Grebosz, M. *J. Colloid Interface Sci.* **2003**, *265*, 214–219.